Divalent ansa-Octaphenyllanthanocenes: Synthesis, Structures, and EuII Luminescence.

Angus Shephard, Aymeric Delon, Sylviane Chevreux, Agathe Martinez, Zhifang Guo, Glen Deacon, Gilles Lemercier, Nathan Mcclenaghan, Gediminas Jonusauskas, Peter Junk, et al.

Divalent *ansa*-Octaphenyllanthanocenes: Synthesis, Structures and Eu^{II} Luminescence

Angus C. G. Shephard,[†] Aymeric Delon,[†,§] Sylviane Chevreux,[§] Agathe Martinez,[§] Zhifang Guo,[†] Glen B. Deacon,[Δ] Gilles Lemercier,[§] Nathan McClenaghan,[$] Gediminas Jonusauskas,[#] Peter C. Junk[†] and Florian Jaroschik[¶*]*

† College of Science and Engineering, James Cook University, Townsville 4811, Australia

§ Université de Reims Champagne-Ardenne, ICMR, UMR 7312, 56187 Reims, France

Δ School of Chemistry, Monash University, Clayton, Vic, 3800 Australia

$ Univ. Bordeaux, CNRS, Bordeaux INP, ISM, UMR 5255, F-33400 Talence, France

Univ. Bordeaux, CNRS, LOMA, UMR 5798, F-33400 Talence, France

¶ ICGM, Univ Montpellier, CNRS, ENSCM, 34090 Montpellier, France

ABSTRACT. Reductive dimerisation of fulvenes using low-valent metal precursors is a straightforward one-step approach to access ethylene-bridged metallocenes. This process has so far mainly been employed with fulvenes carrying one or two substituents in the exocyclic position. In this work, a new synthesis of the unsubstituted exocyclic 1,2,3,4-tetraphenylfulvene (**1**), its full structural characterisation by NMR spectroscopy and single-crystal X-ray diffraction, as well as some photophysical properties and its first use in reductive dimerisation are described. This fulvene reacted with different lanthanoid metals in thf to provide the divalent *ansa*-octaphenylmetallocenes $[Ln(C_5Ph_4CH_2)_2(thf)_n]$ (Ln = Sm, n = 2 (**2**); Ln = Eu, n

= 2 (**3**), Ln = Yb, n = 1 (**4**)). These complexes were characterised by X-ray diffraction, LDI-TOF spectrometry and, in the case of Sm and Yb, by multinuclear NMR spectroscopy showing the influence of the *ansa*-bridge on solution and solid-state structures compared to previously reported unbridged metallocenes. Furthermore, the luminescence properties of the Eu *ansa* complex **3** were studied in solution and the solid state, revealing significant differences with the known octa- and deca-phenyleuropocenes, $[Eu(C_5Ph_4H)_2(dme)]$ and $[Eu(C_5Ph_5)_2]$.

1. INTRODUCTION

Ansa-metallocene complexes of main group, rare earths and early transition metals have been widely studied in the controlled synthesis of polymers, in organic and medicinal chemistry and in small molecule activation.[1] Various bridge sizes have been developed using carbon or heteroelements (Si, P, B, N) in the bridge, with one or two element bridges being the most widely employed.[2] Most literature complexes are based on ancillary Cp, indenyl or fluorenyl ligands in different combinations, but other monoanionic groups such as scorpionates or allyl ligands have also been reported.[3] A certain "*ansa*-effect" has been observed in the stability or reactivity of complexes compared to their non-bridged analogues and can be related to the strain of the bridge or the ligand environment imposed by the bridge.[2a,4]

From a synthetic point of view, salt-metathesis reactions between metal halides and dianionic *ansa* ligands are very common, even though this can potentially lead to alkali-salt inclusion. Recent examples in rare earth chemistry include the synthesis of divalent ethylene-bridged *ansa*-bis(1,3-diphenylcyclopentadienyl) complexes **A-Ln**, including the first structurally characterized divalent Eu *ansa* complex **A-Eu**,[5] the divalent Si-bridged boratabenzene-fluorenyl complexes **B**,[6] and the trivalent carbon-bridged Cp/fluorenyl lanthanoid allyl polymerisation pre-catalysts **C** (Scheme 1a).[7] Alternatively, protolysis reactions of neutral *ansa* proligands with air and moisture sensitive metal-alkyl or amido complexes have been employed

in lanthanoid and group 4 metal chemistry.[8] For substituted or unsubstituted ethylene-bridged metallocenes, the most straightforward synthesis consists in the reductive dimerisation of pentafulvenes using a low-valent metal precursor.[1b,9] This one-step methodology has been applied to a wide range of metals across the periodic system. Seminal work by Edelmann in the 1990s showed the applicability of this process to lanthanoid and group 2 metals, even though no lanthanoid complex from these reactions could be structurally characterised (Scheme 1b).[10] Whereas the calcium chemistry was subsequently explored by Shapiro and others,[1c,2a,11] only one other example exists for lanthanoid metals, namely that reported by Schumann on the reductive dimerisation of acenaphthenes to afford C_2-symmetric *trans-rac-ansa*-lanthanocene complexes $[(\eta^5\text{-}C_{12}H_8)_2Ln(thf)_2]$ (Ln = Sm, Yb) (Scheme 1c).[12]

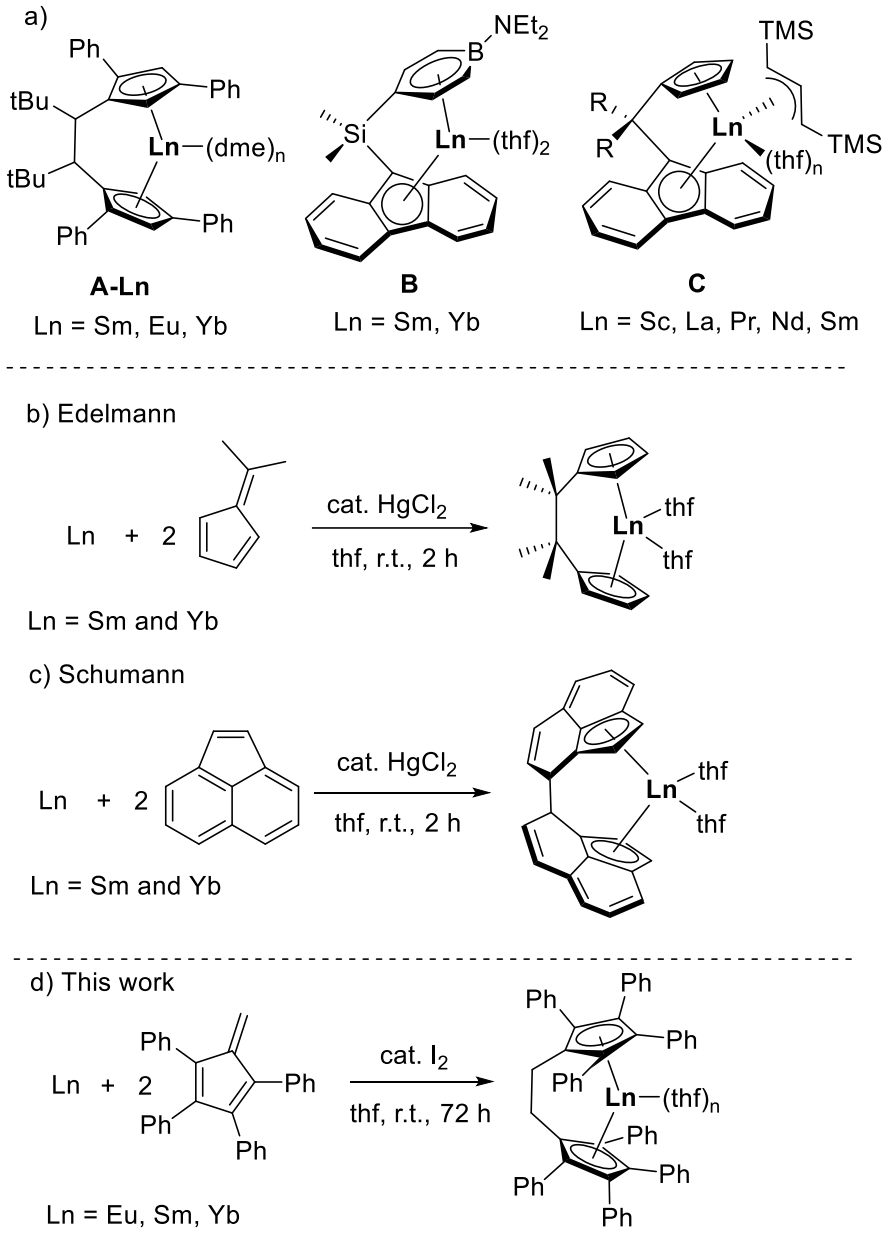

Scheme 1. a) Recent examples of divalent and trivalent rare earth *ansa* complexes;[5-7] b) and c) Reductive dimerisation of fulvenes with lanthanoids;[10a,12] d) this work.

Over the last 15 years, we and others have explored the synthesis, structures and properties of divalent lanthanoid octa and decaphenylmetallocenes $[Ln(C_5Ph_4H)_2(solv)]$ or $[Ln(C_5Ar_5)_2]$ (Yb, Sm, Eu).[13] So far, such divalent complexes have only been synthesised by protolysis of highly reactive lanthanoid benzyl precursors[13e-g] or via metal based reactions using either redox transmetallation/protolysis (RTP)[13a-c] or a methodology involving a selective C-P bond

cleavage.[13d] Classical salt metathesis reactions were hampered by the low reactivity of the bulky and electronically stabilised Cp ligands and have only been successful for the synthesis of trivalent complexes.[14]

These polyarylCp ligands are relatively labile in the divalent metallocenes, leading even to solvent separated ion-pairs (SSIP) in the case of pentaarylCps, such as the structurally characterised $[Yb(thf)_6][C_5Ph_5]_2$.[13a] The reported divalent lanthanocenes showed poor reactivity towards oxidants compared to samarocenes based on alkylCp ligands,[13a,g] and the bright orange-red europocenes revealed promising luminescence properties in solution and the solid state.[13c,f] We therefore wondered what structural influence an *ansa*-bridge could have on such complexes and how it could alter the luminescence properties of the divalent europium complex. 1,2,3,4-Tetraphenylfulvene,[15] which is very stable despite the absence of substituents on the exocyclic position, proved to be a valuable precursor for this study. Whereas its use had previously been restricted to cycloaddition chemistry[15b-d] and very limited coordination chemistry,[15e] we herein report its first application in the reductive dimerisation of lanthanoids providing new divalent *ansa*-metallocenes with intriguing properties (Scheme 1c).

2. METHODS

2.1 General

All manipulations were performed under nitrogen, using standard Schlenk techniques. Lanthanoid metals were from Santoku/Molycorp/Eutectix. Large chunks were filed in the drybox before use. Solvents (thf, toluene, C_6D_6) were pre-dried by distillation over sodium or sodium benzophenone ketyl before being stored under an atmosphere of nitrogen over 3 Å molecular sieves. In all cases, unless specified, ca. 1 mg of I_2 (5 mol%) was used to activate the metal. Infrared spectra (4000–400 cm^{-1}) were obtained as Nujol mulls between NaCl plates with a Nicolet-Nexus FT-IR spectrometer. ^1H and ^{13}C NMR spectra were recorded on a Bruker 400

MHz spectrometer and were referenced against residual solvent peaks. ^{171}Yb NMR spectra were recorded on a Bruker 500 MHz spectrometer with [Yb(C_5Me_5)$_2$(thf)] as external standard. No interpretable NMR spectra could be collected for the highly paramagnetic europium complex **3**. Microanalyses were determined by the Elemental Analysis Service, Macquarie University, and all the samples were sealed in tubes under nitrogen before transport.

2.2 Synthesis

1,2,3,4-tetraphenylfulvene (1)

Method 1: MeLi (20 mL, 1.6 M in Et_2O, 32 mmol) was added to a two-necked round bottom flask equipped with a condenser containing 2,3,4,5-tetraphenylcyclopentadienone (2.0 g, 5.2 mmol). The suspension was heated to 40 ºC for 40 minutes, before quenching with dilute HCl, then extracted with ethyl acetate (2 × 20 mL). The organic fractions were combined and stirred over $MgSO_4$, filtered, and the solvent removed under reduced pressure to yield the desired alcohol as a yellow solid. The yellow solid was dissolved in glacial acetic acid (40 mL) and heated to 140 °C before concentrated HCl (37% aqueous solution, 1.8 mL) was added. The mixture was heated to reflux for two hours then extracted with toluene (2 × 25 mL). The organic fractions were combined and stirred over $MgSO_4$, filtered, and then the solvent was removed under reduced pressure. The obtained dark orange solid was washed with hexanes, and filtered, yielding the fulvene **1** as a bright orange powder (1.82 g, 4.76 mmol, 95%) Crystals of **1** were grown from the slow evaporation of a dichloromethane solution. M.p. 206 °C (lit. 211 °C).[15a] ^{1}H NMR ($CDCl_3$, 400 MHz, 25 ˚C): δ 7.30-6.88 (m, 20H, ArH), 6.04 (s, 2H, CH_2). ^{13}C NMR ($CDCl_3$, 101 MHz, 25 ˚C): δ 152.44 (s), 143.56 (s), 135.06 (s), 133.05 (s), 130.96 (s), 130.29 (s), 127.93 (s), 127.44 (s), 126.63 (s), 126.53 (s), 123.83 (s). IR (ATR, cm^{-1}): 3051 m, 1963 w, 1882 m, 1669 m, 1596 s, 1573 m, 1553 w, 1485 s, 1438 s, 1394 m, 1340 m, 1260 w, 1179 m,

1156 m, 1106 m, 1074 m, 1027 s, 939 m, 907 s, 845 w, 794 m, 767 m, 748 s, 730 s, 693 s, 654 w, 640 w, 618 w, 589 w, 555 w, 542 s, 516 s, 497 m, 476 m, 456 m.

Method 2: A Schlenk flask was charged with caesium carbonate (4.5 eq.), palladium acetate (0.05 eq.), and anhydrous DMF. Freshly cracked methylcyclopentadiene (1 eq.) and bromobenzene (4.5 eq.) were added while stirring. The mixture was heated to 140 ˚C before tri-tertbutylphosphine (0.1 eq.) was added. The mixture was stirred for two days at 140 ˚C before CH_2Cl_2 was added to the mixture. The solution was separated by filtering through celite, and then washed six times with water to remove traces of DMF. The solvent was removed under reduced pressure to yield a mixture of isomers of tetraphenylmethylcyclopentadiene as an orange powder (95%), which was used without further purification. A solution of n-BuLi (2.3 M in hexane, 1.3 eq.) was added at 0 °C to a toluene/thf solution of this mixture of isomers of tetraphenylmethylcyclopentadiene. After 1 h, Ph_3CCl (0.9 eq.) was added and the solution was kept at 5 °C for 12 h. The reaction mixture was quenched with water and extracted with CH_2Cl_2. Evaporation of the combined organic phases and recrystallisation from CH_2Cl_2 at 0°C afforded the fulvene **1** in 90 % yield, which showed the same NMR spectra as with Method 1.

[Sm($C_5Ph_4CH_2$)$_2$(thf)$_2$]·3thf (2)

A Schlenk flask was charged with 1,2,3,4-tetraphenylfulvene (**1**) (0.076 g, 0.20 mmol), freshly filed samarium metal (0.15 g, 1.0 mmol) and a catalytic amount of iodine. Anhydrous thf (5 mL) was added, and the reaction mixture stirred for 72 hours. The solid material was allowed to settle, and the supernatant solution isolated by cannula filtration. The solution was concentrated to ~1 mL and allowed to stand at room temperature, yielding dark brown crystals of **2** (0.035g, 28%). *Anal*. Calc. for $C_{80}H_{84}O_5Sm$ (1275.88 g.mol^{-1}): C, 75.31; H, 6.64. Found: C, 75.32; H, 5.93 %. ^{1}H NMR (400 MHz, C_6D_6) (some signals are flattened out in the baseline due to paramagnetism; small excess of thf present) δ 17.47 (s, 6H), 13.21 (s, 4H, ArH), 5.22 (s,

6H, ArH), 4.92 (s, 10H, ArH), 2.54 (s, 30H, thf), -0.45 (s, 30H, thf), -4.11 (s, 4H, CH_2). ^{1}H NMR (400 MHz, thf/C_6D_6) δ 22.78 (br s, 8H), 12.48 (s, 8H, ArH), 10.50 (s, 4H, ArH), 5.76 (s, 4H, ArH), 5.28 (s, 8H), 1.22 (s, 8H), -2.50 (s, 4H, CH_2). ^{13}C NMR (126 MHz, C_6D_6) δ 175.2 (s), 151.2 (s), 136.7 (s), 131.8 (s), 131.4 (s), 127.9 (s), 126.6 (s), 123.2 (s), 87.0 (s), 67.9 (s), 25.4 (s), -1.6 (s), -29.8 (s), -46.7 (s). IR (Nujol, cm^{-1}): 1593 m, 1305 w, 1260 m, 1154 w, 1072 w, 1025 m, 789 w, 771 w, 723 m, 696 m.

[Eu($C_5Ph_4CH_2$)$_2$(thf)$_2$]·3thf (3)

The synthesis of complex **3** was carried out in the same way as that described for complex **2**, but with 1,2,3,4-tetraphenylfulvene (**1**) (0.200 g, 0.524 mmol), and europium filings (0.230 g, 1.51 mmol) were used in place of samarium. Amber crystals of **3** were grown from ~2 mL of thf at room temperature (0.120 g, 38%). *Anal.* Calc. for $C_{80}H_{84}O_5Eu$ (1277.48 $g.mol^{-1}$): C, 75.21; H, 6.63. Found: C, 75.25; H, 6.65%. IR (Nujol, cm^{-1}): 1593 m, 1574 w, 1308 w, 1260 m, 1176 w, 1153 w, 1096 w, 1069 w, 1020 m, 907 w, 869 m, 789 m, 771 w, 744 m, 695 m, 661 w, 616 w.

[Yb($C_5Ph_4CH_2$)$_2$(thf)]·2.5thf (4)

The synthesis of complex **4** was carried out in the same way as that described for complex **3**, but with ytterbium filings (0.270 g, 1.52 mmol) used in place of europium. Green-brown crystals of **4** were grown from ~2 mL of thf at room temperature (0.095 g, 33%). *Anal.* Calc. for $C_{72}H_{68}O_3Yb$ (1154.35 $g.mol^{-1}$ after loss of one half of a lattice thf): C, 74.91; H, 5.94. Found: C, 74.30; H, 5.518%. ^{1}H NMR (500 MHz, C_6D_6) (loss of 1.5 lattice thf) δ 6.75-7.10 (m, 40H), 3.8 (vbs, 8H, thf), 3.44 (s, 4H, CH_2), 1.50 (vbs, 8H, thf). ^{13}C NMR (126 MHz, C_6D_6) δ 138.8 (s), 138.3 (s), 131.8 (s), 130.8 (s), 130.2 (s), 128.9 (s), 128.8 (s), 127.3 (s), 126.4 (s), 125.0 (s), 124.9 (s), 68.5 (bs, thf) 27.8 (s), 25.8 (bs, thf). ^{171}Yb NMR (88 MHz, C_6D_6) δ 208.4 (bs). ^{171}Yb NMR (88 MHz, thf/C_6D_6) δ 164.5 (bs). IR (Nujol, cm^{-1}): 1944 w, 1882 w, 1802 w, 1595 m,

1574 w, 1342 w, 1261 m, 1176 w, 1155 w, 1100 m, 1071 m, 1027 m, 939 w, 911 m, 865 w, 838 w, 795 w, 788 w, 249 m, 696 s, 628 w, 616 w.

1,2-bis(2,3,4,5-tetraphenylcyclopenta-2,4-dien-1-yl)ethane (5)

From the synthesis of **3**, small colourless crystals of **5** were isolated and characterised by X-ray crystallography. Owing to the low yield, no further useful characterisation was obtained.

2.3 X-ray crystallography

Single crystals coated with viscous hydrocarbon oil were mounted on a cryoloop or a glass fibre. Data for compound **1** were obtained at -173.15 ˚C (100 K) and were measured on a Bruker D8 Venture. The D8 venture was equipped with a Cu microsource ($K\alpha_1$ radiation $\lambda = 1.54056$ Å). Data collection and integration was performed using Bruker Apex2 software. Data for compounds **2-5** were obtained at -150 ˚C (123 K) and were measured on a Rigaku SynergyS diffractometer. The SynergyS operated using microsource Mo-Kα radiation ($\lambda = 0.71073$ Å) and Cu-Kα radiation ($\lambda = 1.54184$ Å). Data processing was conducted using CrysAlisPro.55 software suite.[16] The structures were solved using SHELXS-97 and SHELXS7 and refined by full-matrix least-squares on all F2 data using SHELX2014[17] in conjunction with the X-Seed graphical user interface.[18] All hydrogen atoms were placed in calculated positions using the riding model.

2.4 LDI-TOF

All Matrix-free LDI-MS experiments were performed on a MALDI micro MX mass spectrometer (Waters/Micromass Manchester UK) equipped with a N_2-laser ($\lambda = 337$ nm, 4 ns pulse duration up to 20 Hz repetition rate and max 320 μJ per pulse) in positive ion mode for data acquisition.

2.5 UV-vis and luminescence

Solution measurements of fulvene **1** and complex **3** in toluene: UV-vis and emission spectra were recorded on a Cary 5000 UV-2401PC spectrophotometer and a Varian Cary Eclipse spectrofluorometer, respectively.

Solid state luminescence (powder of complex **3** sealed in a glass capillary under inert atmosphere): The time-resolved luminescence set-up was built as follows : a frequency tripled Nd:YAG amplified laser system (5 ns, 135 mJ at 355 nm from Nd:YAG amplified laser pumping OPO, 10 Hz, Ekspla model NT342B-10-WW); produced tunable excitation pulses in the range 410-2300 nm. Light signals were analysed by a spectrograph (Princeton Instruments Acton model SP2300) coupled with a high dynamic range streak camera (Hamamatsu C7700, sub-1 ns-1 ms). Accumulated sequences of pulses were recorded and treated by HPDTA (Hamamatsu) software to produce maps (wavelength vs delay) of transient emission intensity in the range 300 – 800 nm. Data were further analysed using home-made software developed in LabVIEW 2014 system-design platform and development environment.

3. RESULTS AND DISCUSSION

3.1 Synthesis and characterisation of 1,2,3,4-tetraphenylfulvene

Initially, we used a slightly modified version of the original synthesis of 1,2,3,4-tetraphenylfulvene **1** by adding 1,2,3,4-tetraphenylcyclopentanone to an ethereal MeLi solution (Scheme 2a).[15] After workup, fulvene **1** was obtained in high yields by refluxing the obtained cyclopentadienol in HCl/glacial acetic acid, followed by recrystallisation from dichloromethane at 0 °C. We then investigated an alternative synthesis using a modified Ogino-Erker approach, i.e. starting from a lithium tetraphenylmethylcyclopentadienide and hydride abstraction with a trityl salt (Scheme 2b).[19] Previously, this synthesis has only been applied to pentamethylcyclopentadiene (Cp*H) to access 1,2,3,4-tetramethylfulvene. The starting compound, methyltetraphenylcyclopentadiene (Cp'H),[20] was synthesised in high yield using

the Pd catalysed arylation of methylcyclopentadiene with tBu_3P as ligand and bromobenzene as an aryl source (Scheme 2b).[21] This is the first report on the use of this methodology with a substituted cyclopentadiene, previously either the parent cyclopentadiene C_5H_6 or Cp_2ZrCl_2 was employed.[21] Subsequently, Cp'H was metallated using nBuLi and addition of trityl chloride to the *in situ* formed LiCp' provided fulvene **1**, again in very good yields. As the Pd catalysed methodology is applicable to a wide range of aryl groups,[21] this approach offers the prospect of accessing various modified 1,2,3,4-tetraarylfulvenes.

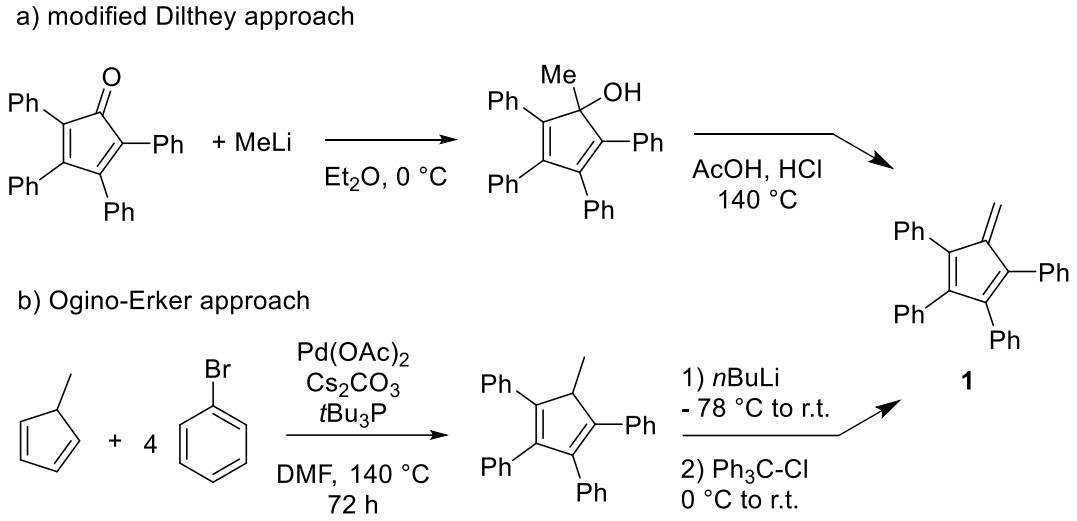

Scheme 2. Two complementary synthetic pathways to 1,2,3,4-tetraphenylfulvene **1**.

Fulvene **1** was characterised by ^1H and ^{13}C NMR spectroscopy and the data were compared to the parent fulvene C_6H_6 and the 6,6-dicyano-substituted tetraphenylfulvene (see SI, Table S1).[22,23] From the comparison with the parent fulvene the influence of the phenyl groups on the fulvene ring can be assessed. As mentioned in previous NMR studies on various pentafulvenes,[22c] ring substituents have only a minor influence on chemical shifts. On the other hand, replacing the two H groups in the exocyclic position of **1** with cyano groups clearly shows a dramatic influence on the shifts of the exocylic carbon atoms. The UV-vis spectrum of **1** shows a sharp absorption at 284 nm with a shoulder at 316 nm and a weak broad absorption at

457 nm (Figure S24). Upon excitation of **1** at 355 nm, a broad emission peak at 445 nm was observed, similar to 1,3-diphenyl-6-t-butyl (460 nm) and 1,3-diphenyl-6-fluorenylfulvene (451 nm).[24] The Stokes shift of 5800 cm^{-1} in **1** (between 348 and 438 nm) is much larger than the ones observed and reported in a series of 1,3,6-triarylfulvenes (around 3500 cm^{-1}).[24]

Single crystals of **1** suitable for XRD studies (Figure 1) were obtained by slow evaporation of a dichloromethane solution. The compound shows bond lengths and angles comparable to other fulvenes, such as 1,2,3,4,6-pentaphenylfulvene.[25] No significant changes were observed compared to the microwave structure of the parent fulvene (see SI, Table S1).[22a] The electronic influence on structural parameters can be observed by comparison with the 6,6-dicyano analogue, exhibiting a longer exocyclic C=C bond due to the more electron-withdrawing groups.[23]

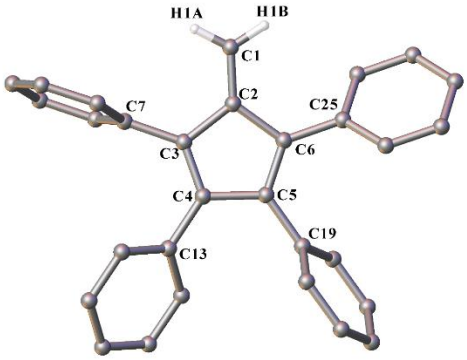

Figure 1. Molecular structure of 1,2,3,4-tetraphenylfulvene **1**.

3.2 Reductive dimerisation with lanthanoids

Even though the reductive dimerisation of fulvenes by lanthanoid metals should be a stoichiometric process, a large panel of reaction conditions has been reported in the literature for different metals, most of them making use of an excess of the metal, and utilising various activation methods (e.g., iodine, amalgamation).[10,12]

Screening different metal to fulvene ratios, we found that the best results when synthesising the lanthanoid *ansa* complexes [Ln($C_5Ph_4CH_2$)$_2$(thf)$_n$] (Ln =, Sm (**2**) n = 2, Eu (**3**) n = 2, and Yb (**4**) n = 1) were obtained from the reaction of an excess of Ln metal (4 equivalents, activated with a crystal of iodine, ca. 5 mol %) with two equivalents of fulvene **1** and stirring the reaction mixture in thf for 72 hours at room temperature (Scheme 3). An insoluble precipitate, possibly some polymeric material, formed during the reaction, regardless of stoichiometry, and could not be identified despite numerous attempts. After removing this precipitate by filtration, the solution was concentrated under reduced pressure, and the *ansa* complexes **2-4** crystallised from the concentrated solutions in low to moderate yields. Single crystals of dark-red [Sm($C_5Ph_4CH_2$)$_2$(thf)$_2$]·3thf (**2**), bright amber [Eu($C_5Ph_4CH_2$)$_2$(thf)$_2$]·3thf (**3**), and green-brown [Yb($C_5Ph_4CH_2$)$_2$(thf)]·2.5thf (**4**) suitable for XRD studies were obtained from concentrated thf solutions upon standing at room temperature. When the reaction was conducted with Tm metal a yellow solution was observed and LDI-MS of the crude reaction mixture confirmed the presence of a [Tm($C_5Ph_4CH_2$)$_2$]$^+$ species (see SI, Fig. S18), but no well-characterised complex could be isolated. During recrystallisation attempts of complex **3**, small amounts of the *ansa* proligand ($C_5Ph_4HCH_2$)$_2$ (**5**), formed by adventitious hydrolysis, were obtained and identified by XRD (see SI, Fig. S23), however, the NMR analysis of **5** was hampered by the presence of a large number of regioisomers in the Cp rings.

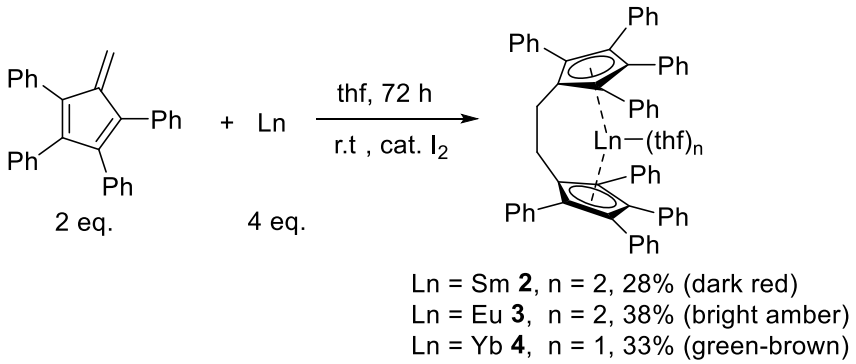

Scheme 3. Synthesis of *ansa*-octaphenylmetallocene complexes of Sm (**2**), Eu (**3**), and Yb (**4**).

The purity of the new complexes **2-4** was confirmed by elemental analyses, and where possible, NMR spectroscopy.

Complexes **2-4** were also characterised by LDI-TOF mass spectrometry, a powerful tool initially used for the characterisation of poorly soluble decaphenylmetallocenes of Yb, Ca and Ba.[13a] Analysis of the new Ln *ansa* complexes showed a signal at m/z 916.6 for **2**, 917.5 for **3**, and 938.6 for **4**, in perfect agreement with the calculated values, and also the correct isotope distributions were observed (see SI, Fig. S15-S17).

Multinuclear NMR spectroscopy of complexes **2** and **4** revealed the influence of the *ansa*-bridge on the solution structure compared to the corresponding octa- and deca-phenylmetallocenes. In the ^{1}H NMR spectrum of the diamagnetic complex **4**, the signal for the CH_2 groups of the *ansa*-bridge appears at 3.44 ppm and the thf peaks are very broad. The ^{171}Yb NMR spectrum of **4** in C_6D_6 at r.t. shows a broad signal at 163 ppm and in a thf/C_6D_6 mixture at 208 ppm, which is in the usual area for Yb-sandwich complexes.[26] The signal for the non-bridged octaphenylytterbocene [Yb($C_5Ph_4H)_2$(thf)] was previously observed at 116 ppm in thf/C_6D_6.[13b]

^{1}H and ^{13}C NMR spectra of the paramagnetic Sm *ansa* complex **2** provided some interesting insights compared to the non-bridged octaphenylsamarocenes Sm($C_5Ph_4H)_2$ and Sm(C_5Ph_2(*p*-tol)$_2)_2$.[13c] As previously shown, the phenyl groups next to the H on the C_5Ph_4H ring are more impacted by the paramagnetic metal center than the phenyl groups further away and the shifts are influenced by the solvent (Fig. 2). Similarly, in **2** the phenyl groups next to the *ansa*-bridge show broad signals at 17.47 and 13.21 ppm in a 8:4 ratio in C_6D_6 (Fig. 2c) whereas in C_6D_6/thf-d_8 three signals were observed at 22.78, 12.48 and 10.50 in a 8:8:4 ratio (Fig. 2d) very close to the unbridged Sm($C_5Ph_4H)_2$ in neat C_6D_6 (Fig. 2a). A significant difference concerns the other phenyl rings, which were nearly not paramagnetically impacted in the unbridged complexes but

are strongly influenced in the *ansa* complex at 5.76, 5.28 and 1.22 ppm in a 4:8:8 ratio. These data were confirmed by ^{1}H-^{1}H COSY experiments. The signal for the CH_2 of the bridge appears between -2.50 and -4.25 ppm, depending on the solvent, shifted in the same direction as the ring C-H in $Sm(C_5Ph_4H)_2$ (-9.58 ppm). The amount of thf present in the NMR tube had a huge impact in the unbridged complex, especially on the ring C-H (Fig. 2a,b), whereas for **2** much less influence was observed (Fig. 2c,d). This might be explained by a higher flexibility of the C_5Ph_4H ligand compared to the *ansa* ligand, as the former could accommodate more thf molecules at the metal center in solution. In the ^{13}C spectrum of **2**, signals for all carbon atoms were observed in the range from -50 to 180 ppm, which is a slightly smaller range than for the unbridged complex (-86 to 191 ppm). The signal for the CH_2 groups of the bridge was found at 87 ppm.

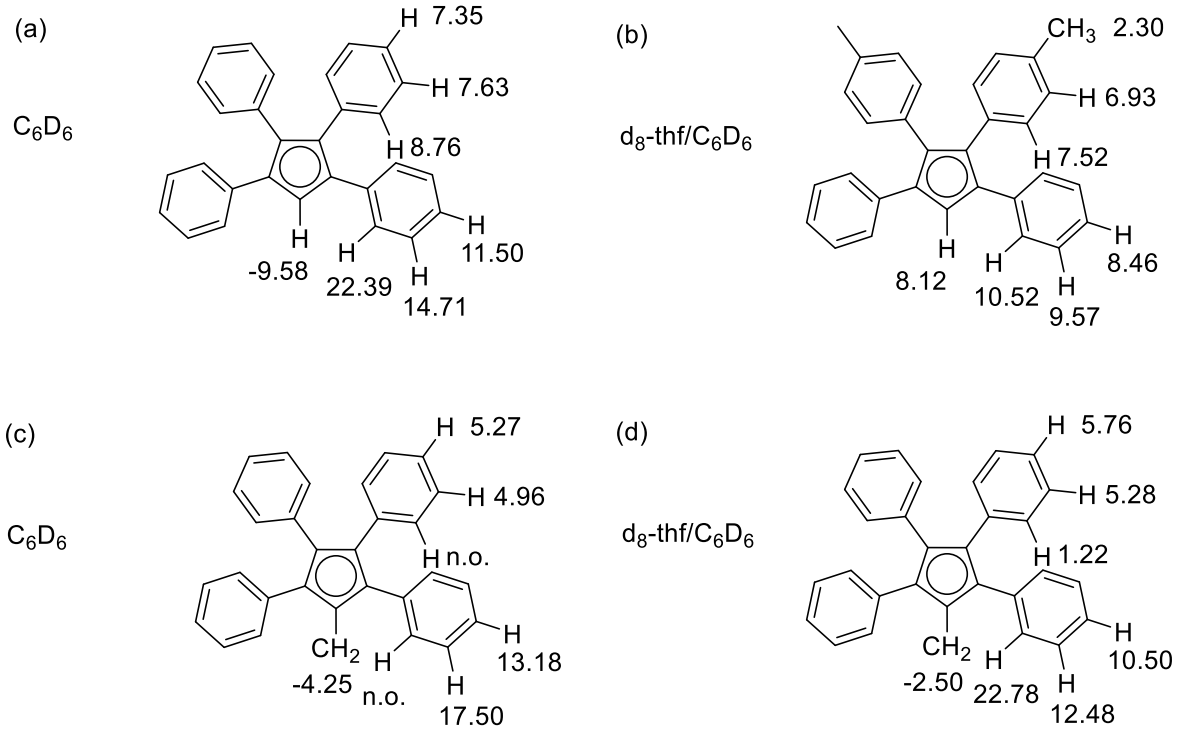

Figure **2**. Comparison of ^{1}H NMR data of unbridged Sm complexes (a, b)[13c] and the new Sm *ansa* complex **2** (c,d) in different solvent systems.(n.o. = not observed).

X-ray crystal structures of **2-4**

Single crystals suitable for X-ray diffraction were obtained for complexes **2-4.** Their ORTEP diagrams are shown below (Fig. 3 and 4 and S20) and selected bond lengths and angles of complexes **2-4** are summarised in Table 1 alongside comparisons with other *ansa* complexes, and untethered sandwich complexes. The angle of Cn(1)-M-Cn(2) (γ) represents the angle between the vectors from the metal to the ring centroids, whilst the angle of Cn(1)-Cn(2) (β) represents the angle between the vectors normal to the ring centroids. These parameters are particularly useful, as the absolute value of difference between these parameters (i.e. $|\gamma - \beta|$) reflects the amount of slippage of the metal from a standard η^5 mode of coordination to each ring.[2a] These parameters are illustrated in Figure 5, and the values summarised in Table 1.

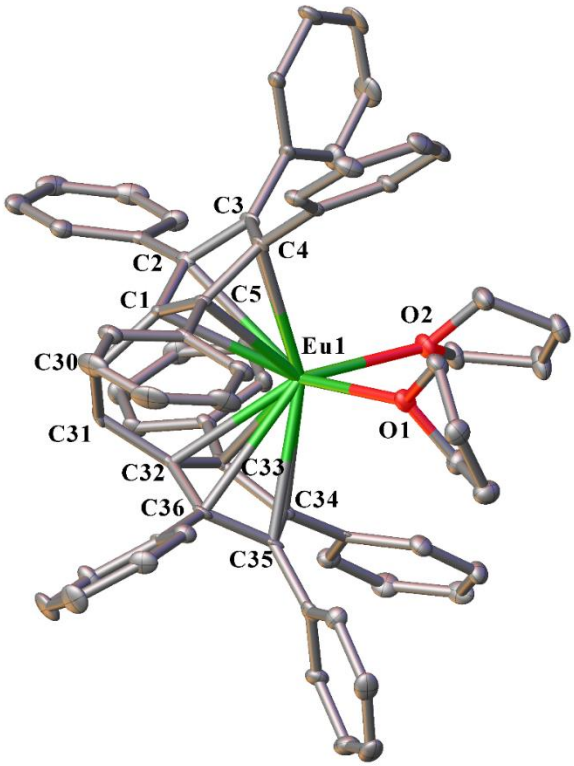

Figure **3** – ORTEP diagram of complex **3** (also representative of **2**) showing atom-numbering scheme for relevant atoms. Thermal ellipsoids are drawn at the 50% probability level. Hydrogen

atoms and lattice thf are omitted for clarity. Selected bond lengths of **3** (with data for **2** in square brackets) (Å): Ln(1)-Cn(1) 2.616(2) [2.6265(2)], Ln(1)-Cn(2) 2.6246(18) [2.627(3)], Ln(1)-O(1) 2.605(3) [2.646(4)], Ln(1)-O(2) 2.628(3) [2.613(4)].

The Sm complex **2** and Eu complex **3** are isomorphous, both crystallising in the monoclinic space group $P2_1$ and having two thf molecules coordinated to the metal centre (Figure 3). The cyclopentadienyl rings of **2** and **3** display similar Cn(1)-Ln(1)-Cn(2) angles of 115.83(7)˚ and 115.78(9)˚ respectively, owing to their similar ionic radii. The *ansa* complexes **2** and **3** exhibit longer metal to centroid bond lengths than those observed for their octaphenyl counterparts (**2**: Sm-Cn = 2.625(2) and 2.672(3) vs. octaphenylsamarocene: Sm-Cn = 2.573 and 2.564 Å, and **3**: Eu-Cn = 2.616(2) and 2.6246(18) vs. the dme solvate of octaphenyleuropocene: Eu-Cn = 2.599 and 2.596 Å) (summarised in Table 1). In the case of the Sm complexes, this difference in lengths can be partly explained by the change in coordination numbers from seven to eight, and dme is less bulky than two thf molecules. The angle of the Cp rings in complex **2** about the Sm metal centre (115.83(7)˚) is much smaller than that observed for octaphenylsamarocene (151.47 ˚),[13c] again demonstrating the influence of the tether on the interplanar angle.

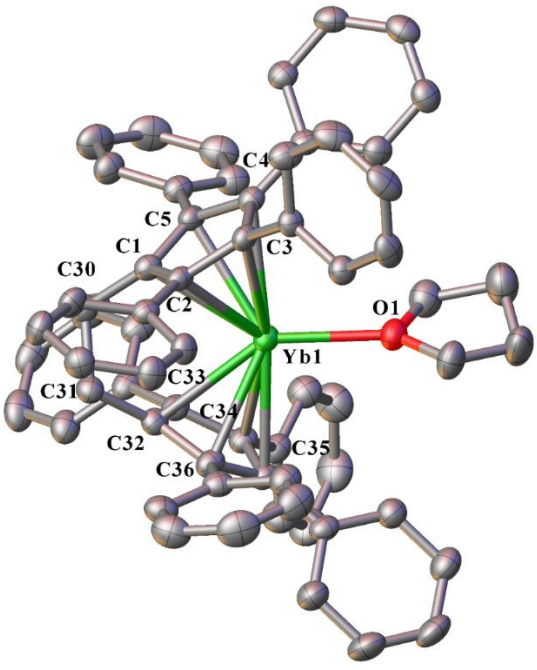

Figure **4** – ORTEP diagram of complex **4** showing atom-numbering scheme for relevant atoms. Thermal ellipsoids are drawn at the 50% probability level. Hydrogen atoms and lattice thf are omitted for clarity. Selected bond lengths of **4** (Å): Yb(1)-Cn(1) 2.4105(14), Yb(1)-Cn(2) 2.4151(14), Yb(1)-O(1) 2.389(2).

Complex **4** crystallised in the monoclinic *C*2/*c* space group, whereby the Yb centre is coordinated to the two cyclopentadienyl rings, and one molecule of thf (Figure 4). The planar angle between the two cyclopentadienyl rings with respect to the ytterbium centre is 124.61(5)˚, much smaller than the corresponding angle of octaphenylytterbocene (150.84(9)˚),[13b] which demonstrates the strong influence of the CH_2-CH_2 tether on the interplanar angle. The Yb-Cn bond lengths observed for **2** are consistent with those reported for the analogous thf-complexed octaphenylytterbocene (Yb-Cn = 2.440(3) and 2.448(3) Å)[13b] (summarised in Table 1), and slightly longer than that of decaphenylytterbocene (Yb-Cn = 2.3710(12) and 2.3814(13) Å for the ytterbocene with lattice C_6D_6,[13d] and 2.3711(10) Å for the solvent-free ytterbocene).[13a] The differences between **4** and [Yb(C_5Ph_5)$_2$] are consistent with the difference in coordination number (7 to 6).

Table 1 also summarises the comparison of various parameters between the recently reported divalent *ansa* complexes **A-Ln** synthesised by Balaich et al.[5] (see Scheme 1) and our new complexes. The reported **A-Ln** complexes are more open (smaller Cp-M-Cp angle) despite the presence of only two phenyl rings on the Cp ligand, however, this could be related to the presence of two dme molecules in **A-Sm**, **A-Eu** (10-coordination) and one dme in **A-Yb** (8-coordination) vs only two thf in complexes **2** and **3** (8-coordination) and one thf in complex **4** (7-coordination). The ring slippage is significantly larger in **2-4** as is the twist angle of the ethylene bridge. These parameters may indicate a stronger steric crowding in complexes **2-4** caused by the four phenyl groups on the Cp ligand, and despite the presence of the two bulky tBu groups on the tether in **A-Ln**.[5]

Table 1. Comparison of *ansa* complexes (**2-4**) with unbridged cyclopentadienyl based lanthanoid complexes[13a-d] and *ansa* complexes **A-Ln**.[5]

Parameter	**2**	$Sm(C_5Ph_4H)_2(thf)$	**A-Sm**	**3**	$Eu(C_5Ph_4H)_2(dme)$	$Eu(C_5Ph_5)_2$	**A-Eu**	**4**	$Yb(C_5Ph_4H)_2(thf)$	$Yb(C_5Ph_5)_2$	**A-Yb**
M-Cn(1)	2.625(2)	2.5733(19)	2.6756(10)	2.616(2)	2.5963(18)	2.4890(17)	2.6822(11)	2.4105(14)	2.448(3)	2.3711(10)	2.399(2)
M-Cn(2)	2.627(3)	2.5642(18)	2.6756(10)	2.6246(18)	2.5994(18)	2.4890(17)	2.6822(11)	2.4151(14)	2.440(3)	2.3711(10)	2.381(2)
M-O(1)	2.646(4)	2.488(3)	2.6682(15)	2.605(3)	2.547(3)	-	2.696(2)	2.389(2)	2.369(5)	-	2.452(4)
M-O(2)	2.613(4)	-	2.7101(17)	2.628(3)	2.579(3)	-	2.649(2)	-	-	-	2.421(4)
Cn(1)-M-Cn(2) (γ)	115.78(9)	151.47(6)	104.83(4)	115.83(7)	128.62(5)	180.00(0)	104.48(6)	124.61(5)	150.84(9)	180.00(0)	115.95(7)
Cn(1)-Cn(2) (β)	112.0(2)	152.61(16)	104.80(13)	111.72(19)	122.67(15)	-	104.58(14)	120.48(13)	151.4(2)	-	113.13(19)
Slippage ($\|\gamma - \beta\|$)	3.78	1.14	0.03	4.11	5.95	-	0.10	4.13	0.56	-	2.82
Ethylene Bridge Twist	59.7(6)	-	37.0(4)	60.1(5)	-	-	36.6(5)	59.5(4)	-	-	47.4(5)

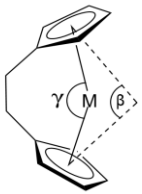

Figure 5 - Visual representation of geometric parameters, γ and β, in a generic C_2 *ansa* complex.

3.3 **Luminescence studies of divalent Eu complex 3**

Molecular divalent europium complexes have recently gained renewed interest for their luminescence properties, especially as the emission can vary in energy (from blue to red), demonstrated with a range of organic[27] or inorganic ligands[28] or host lattices.[29] This has led to applications in light-emitting devices, sensing and catalysis.[30] Divalent europium shows strong broad band luminescence due to transitions between the lowest excited $[Xe]4f^6 5d^1$ configuration of the Eu^{II} ion and the $[Xe]4f^7$ ground state.[31] While the interaction of the 4f orbitals with their surrounding ions is weak, the 5d orbitals are influenced by the ligand field and therefore the $4f^7$–$4f^6 5d^1$ electronic transitions are influenced by the chemical environment of Eu^{II}. As a result, the emission wavelengths, lifetimes and quantum yields of divalent europium can vary in energy depending on the ligands, lattice and nature of any counter-ions. Whereas emission for complexes based on Cp and COT ligands is generally found in the orange-red spectral range,[13c,f,27f-h] inorganic halide or pseudo halide complexes often emit in the blue,[28] including the recent NHC complex $[EuI_2(IMes)(thf)_3]$ and the strongly emissive aza-cryptand complexes.[27a-e] The bulky CNT sandwich complex $[Eu(C_9H_9)_2]$ showed luminescence in the green region[27h] and the air-stable trispyrazolylborate based complexes $[Eu(Tp)_2]$ showed emission from yellow to orange-red depending on the substitution.[27i,j] The bulky amido ligands afforded near linear complexes $[Eu(NR_2)_2]$ ($R = Si(^iPr)_3$) or trigonal planar complexes [K(2.2.2-cryptand)][$Ln(NR'_2)_3$] ($R' = Si(tBuMe_2)$) exhibiting strong and long-lived emission in the green and yellow regions.[27k,l] Solvents and counter-ions[32] can significantly alter emission properties and very recently the temperature influence was shown,[33] for example in the $[Cp^*Eu(BH_4)(thf)_2]_2$ complex, making this the first organometallic Eu^{II}-based optical thermometer.[33a]

The luminescence properties of the new divalent *ansa* Eu complex **3** were investigated. In toluene, complex **3** showed a maximum emission in the deep red region at 720 nm after

excitation at 359 nm (see SI, Fig. S25), which is considerably red-shifted compared to the previously reported orange-red emitting penta- and tetraphenyl sandwich complexes (616 and 645 nm respectively).[13c] To date, only [EuCp*$_2$(Et_2O)] has been reported to emit at even higher wavelengths (730 nm).[27g] Broadband Vis-NIR emitters are currently an active research field.[30c] In the solid state, the red-shift of **3** was less pronounced with a broad emission band whose maximum is at 685 nm (see Figure 6). The excitation spectrum has two broad bands at 360 and 440 nm, close to the one for decaphenyleuropocene (345 and 420 nm) (see SI, Fig. S26). From these values, a large Stokes shift of 8100 and 7700 cm^{-1} can be estimated for **3** and [Eu(C_5Ph_5)$_2$], respectively. It is noteworthy that no evidence of structural re-organisation within the luminescent complex upon excitation is noted, as no emission spectral shifting is observed during the emission.

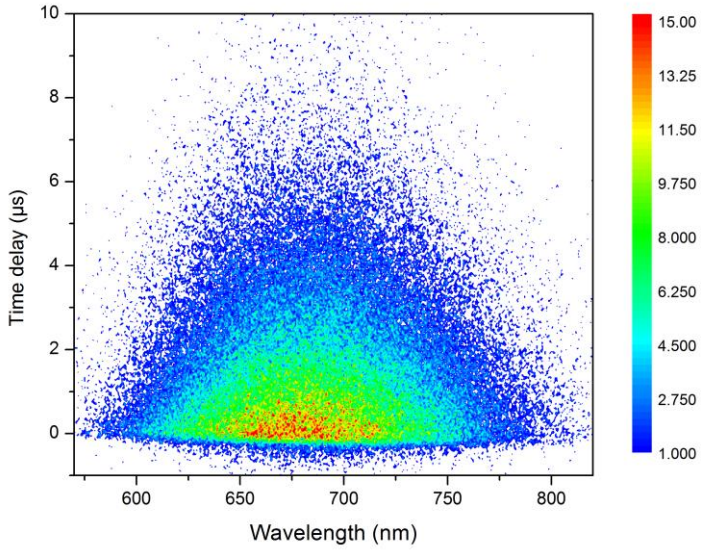

Figure **6**. Time-resolved photoluminescence spectrum of solid **3** (λ_{ex} = 532 nm). LUT/ colored scale bar denotes relative intensity (arbitrary units).

The apparent increased ligand field effect of the *ansa* ligand on the d-orbitals of europium and consequent bathochromic effect on the emission wavelengths with respect to the non-

bridged complexes seems not to be in good agreement with the crystallographic data.[32a] Actually, the Eu-Ct distances significantly increase when going from the pentaphenyl to the tetraphenyl and then to the *ansa* complex (2.489 vs 2.598 vs 2.620 Å). However, it is also very probable that the presence of one dme or two thf molecules in the unbridged and bridged octaphenyleuropocenes could significantly influence the emission energy, as well as the Cp ligand-metal distance and geometry. Interestingly, the luminescence lifetime of the new *ansa* complex in the solid state was considerably longer (2.14 μs) than in the penta- and tetraphenyl complexes (0.55 and 1.07 μs).[13c] To date the longest lifetimes have been determined for the amide complex $[Eu(NR_2)_2]$ ($R = Si(^iPr)_3$) with up to 50 μs,[27k] whereas most other complexes are usually around or below 1 μs.

4. CONCLUSION

Three new divalent *ansa*-bridged octaphenyllanthanocene complexes $[Ln(C_5Ph_4CH_2)_2(thf)_n]$ (Ln = Sm, n = 2 (**2**); Ln = Eu, n = 2 (**3**), Ln = Yb, n = 1 (**4**)) were synthesised by straightforward reductive dimerisation of 1,2,3,4-tetraphenylfulvene with iodine activated lanthanoid metals. Full characterisation of these complexes by NMR, LDI-TOF and XRD revealed a significant effect of the *ansa*-bridge on the geometry and the electronic parameters compared to previously reported unbridged octa- and deca-phenylmetallocene complexes. Especially, the luminescence studies on the divalent Eu complex **3**, which is among the most red-shifted emitters, shows ligand tethering to be an additional means to regulate luminescence. Reactivity studies of these new complexes towards small molecule activation are underway. The much more open coordination sphere around the metal, thanks to the ansa-bridge, should make them more reactive compared to the non-bridged octa- and especially deca-phenylmetallocenes which lack considerable reactivity towards most electrophiles.[13a,g] Furthermore, the readily available and tunable tetraphenylfulvenes are currently under investigation to access non-symmetrical *ansa* ligands with one bulky and one smaller coordination site for selective catalysis purposes.

ASSOCIATED CONTENT

Supporting Information. ORTEP structures of compounds **1-5** (CCDC 2252140-2252144). Multinuclear NMR spectra, IR spectra, LDI-TOF MS spectra, X-ray data and photophysical measurements are provided.

The following files are available free of charge.

supplementary information (PDF) with NMR, IR, LDI-TOF MS spectra, X-ray data and luminescence measurements

AUTHOR INFORMATION

Corresponding Author

*peter.junk@jcu.edu.au, * florian.jaroschik@enscm.fr

Present Addresses

†Sylviane Chevreux : Chimie ParisTech, PSL University, UMR CNRS 8247, Institut de Recherche de Chimie Paris, 75005 Paris, France

Author Contributions

The manuscript was written through contributions of all authors. All authors have given approval to the final version of the manuscript.

Funding Sources

ARC (DP190100798 and DP230100112)

Region Grand-Est (France) EURO2LUM

Notes

The authors declare no conflict of interest.

ACKNOWLEDGMENT

ACGS would like to acknowledge the Australian Government's support of this research through an Australian Government Research Training Program scholarship. AD thanks the Région Grand Est (France) and the JCU for a PhD scholarship (project EURO2LUM). The CNRS and the University of Reims Champagne-Ardenne are acknowledged for financial support. The authors acknowledge support by the Australian Research Council (DP190100798 and DP230100112). Part of this work was conducted using the MX1 beamline at the Australian Synchrotron, which is part of ANSTO,[34] and we thank Dr. Jun Wang for collection of X-ray data. Dr. Dominique Harakat and Mrs. Carine Machado are thanked for LDI-TOF measurements.

REFERENCES

(1) (a) Rodrigues, A.-S.; Kirillov, E.; Carpentier, J.-F. Group 3 and 4 Single-Site Catalysts for Stereospecific Polymerization of Styrene. *Coord. Chem. Rev.* **2008**, *252,* 2115–2136. (b) Strohfeldt, K.; Tacke, M. Bioorganometallic Fulvene Derived Titanocene Anti-Cancer Drugs. *Chem. Soc. Rev.* **2008**, *37*, 1174−1187. (c) Kessler, M.; Hansen, S.; Godemann, C.; Spannenberg, A.; Beweries, T. Synthesis and Structures of Ansa-Titanocene Complexes with Diatomic Bridging Units for Overall Water Splitting. *Chem. - Eur. J.* **2013**, *19*, 6350−6357. (d) Wirtz, L.; Lambert, J.; Morgenstern, B.; Schäfer, A. Cross-Dehydrocoupling of Amines and Silanes Catalyzed by Magnesocenophanes. *Organometallics* **2021**, *40,* 2108–2117.

(2) (a) Shapiro, P. J. The Evolution of the Ansa-Bridge and Its Effect on the Scope of Metallocene Chemistry. *Coord. Chem. Rev.* **2002**, *231*, 67−81. (b) Herbert, D. E.; Mayer, U. F. J.; Manners, I. Strained Metallocenophanes and Related Organometallic Rings Containing π-Hydrocarbon Ligands and Transition-Metal Centers. *Angew. Chem. Int. Ed.* **2007**, *46*, 5060–5081.

(3) (a) Braunschweig, H.; Breitling, F. M. Constrained Geometry Complexes—Synthesis and Applications. *Coord. Chem. Rev.* **2006**, *250*, 2691–2720. (b) Dabringhaus, P.; Schorpp, M.; Scherer, H.; Krossing, I. A Highly Lewis Acidic Strontium *Ansa* -Arene Complex for Lewis Acid Catalysis and Isobutylene Polymerization. *Angew. Chem. Int. Ed.* **2020**, *59*, 22023–22027. (c) Otero, A.; Fernández-Baeza, J.; Antiñolo, A.; Tejeda, J.; Lara-Sánchez, A.; Sánchez-Barba, L.; Rodríguez, A. M.; Maestro, M. A. An Unprecedented Hybrid Scorpionate/Cyclopentadienyl Ligand. *J. Am. Chem. Soc.* **2004**, *126*, 1330–1331. (d) Deacon, G. B.; Forsyth, C. M.; Junk, P. C. η^6:η^6 Coordination of Tetraphenylborate to Ytterbium(II): A New Class of Lanthanoid *Ansa* -Metallocenes. *Eur. J. Inorg. Chem.* **2005**, *2005*, 817–821. (e) Rodrigues, A.-S.; Kirillov, E.; Lehmann, C. W.; Roisnel, T.; Vuillemin, B.; Razavi, A.; Carpentier, J.-F. Allylansa-Lanthanidocenes: Single-Component, Single-Site Catalysts for Controlled Syndiospecific Styrene and Styrene–Ethylene (Co)Polymerization. *Chem. - Eur. J.* **2007**, *13*, 5548–5565.

(4) (a) Wang, B. Ansa-Metallocene Polymerization Catalysts: Effects of the Bridges on the Catalytic Activities. *Coord. Chem. Rev.* **2006**, *250*, 242–258. (b) Zachmanoglou, C. E.; Docrat, A.; Bridgewater, B. M.; Parkin, G.; Brandow, C. G.; Bercaw, J. E.; Jardine, C. N.; Lyall, M.; Green, J. C.; Keister, J. B. The Electronic Influence of Ring Substituents and Ansa Bridges in Zirconocene Complexes as Probed by Infrared Spectroscopic, Electrochemical, and Computational Studies. *J. Am. Chem. Soc.* **2002**, *124*, 9525–9546. (c) Lewin, J. L.; Woodrum, N. L.; Cramer, C. J. Density Functional Characterization of Methane Metathesis in *Ansa*-[Bis(η^5-2-Indenyl)Methane]ML Complexes [M = Sc, Y, Lu; L = CH_3, $CH_2C(CH_3)_3$]. *Organometallics* **2006**, *25*, 5906–5912.

(5) Adas, S. K.; Balaich, G. J. Sodium Naphthalenide Reduction of 1,3–diphenyl–6–(Tert-Butyl) Fulvene: Stabilizing Eu^{2+} with a Sterically Demanding Ansa–ligand Framework. *J. Organomet. Chem.* **2018**, *857*, 200–206.

(6) Wang, C.; Xiang, L.; Leng, X.; Chen, Y. Synthesis and Structure of Silicon-Bridged Boratabenzene Fluorenyl Rare-Earth Metal Complexes. *Organometallics* **2016**, *35*, 1995–2002.

(7) Laur, E.; Louyriac, E.; Dorcet, V.; Welle, A.; Vantomme, A.; Miserque, O.; Brusson, J.-M.; Maron, L.; Carpentier, J.-F.; Kirillov, E. Substitution Effects in Highly Syndioselective Styrene Polymerization Catalysts Based on Single-Component Allyl *Ansa*-Lanthanidocenes: An Experimental and Theoretical Study. *Macromolecules* **2017**, *50*, 6539–6551.

(8) Dash, A. K.; Razavi, A.; Mortreux, A.; Lehmann, C. W.; Carpentier, J.-F. Amine Elimination Reactions between Homoleptic Silylamide Lanthanide Complexes and an Isopropylidene-Bridged Cyclopentadiene−Fluorene System. *Organometallics* **2002**, *21*, 3238–3249.

(9) (a) Preethalayam, P.; Krishnan, K. S.; Thulasi, S.; Chand, S. S.; Joseph, J.; Nair, V.; Jaroschik, F.; Radhakrishnan, K. V. Recent Advances in the Chemistry of Pentafulvenes. *Chem. Rev.* **2017**, *117*, 3930–3989. (b) Eisch, J. J.; Owuor, F. A.; Shi, X. New Syntheses of Ansa-Metallocenes or Unbridged Substituted Metallocenes by the Respective Reductive Dimerization of Fulvenes with Group 4 Metal Divalent Halides or with Group 4 Metal Dichloride Dihydrides. *Polyhedron* **2005**, *24*, 1325−1339. (c) Oziminski, W. P.; Krygowski, T. M.; Fowler, P. W.; Soncini, A. Aromatization of Fulvene by Complexation with Lithium. *Org. Lett.* **2010**, *12*, 4880–4883. (d) Oziminski, W. P. Structural Motifs, Thermodynamic Properties, Bonding and Aromaticity of Sandwich Complexes Formed by Alkaline Earth Metals with Pentafulvene. A Theoretical Approach. *J. Organomet. Chem.* **2012**, *708–709*, 10–17.

(10) (a) Recknagel, A.; Edelmann, F. T. One-Step Synthesis of Organolanthanide(II) Complexes from the Metal. *Angew. Chem. Int. Ed. Engl.* **1991**, *30*, 693–694. (b) Rieckhoff, M.; Pieper, U.; Stalke, D.; Edelmann, F. T. Ansa-Metallocenes of Calcium and Strontium One-Pot Synthesis of Organometallic Complexes of the Heavier Alkaline Earth Metals. *Angew. Chem.*

Int. Ed. Engl. **1993**, *32*, 1079–1081. (c) Edelmann, F. T.; Rieckhoff, M.; Haiduc, I.; Silaghi-Dumitrescu, I. ansa-Metallocenderivate des Samariums und Ytterbiums mit "weichen" Donorliganden. *J. Organomet. Chem.* **1993**, *447*, 203-208.

(11) (a) Baguli, S.; Mondal, S.; Mandal, C.; Goswami, S.; Mukherjee, D. Cyclopentadienyl Complexes of the Alkaline Earths in Light of the Periodic Trends. *Chem. – Asian J.* **2022**, *17*, e202100962. (b) Sinnema, P.-J.; Shapiro, P. J.; Höhn, B.; Bitterwolf, T. E.; Twamley, B. Calcium-Mediated Fulvene Couplings. 1. A Survey of 6,6-Dialkylfulvenes for the Formation of Bridged and Unbridged Calcocenes. *Organometallics* **2001**, *20*, 2883–2888.

(12) Fedushkin, I. L.; Dechert, S.; Schumann, H. Stereoselective Formation of C2-Symmetric Ansa-Lanthanocenes by Reductive Coupling of Acenaphthylene with Activated Ytterbium or Samarium. *Angew. Chem. Int. Ed.* **2001**, *40*, 561–563.

(13) (a) Deacon, G. B.; Forsyth, C. M.; Jaroschik, F.; Junk, P. C.; Kay, D. L; Maschmeyer, T.; Masters, A. F.; Wang, J.; Field, L. D. Accessing Decaphenylmetallocenes of Ytterbium, Calcium, and Barium by Desolvation of Solvent-Separated Ion Pairs: Overcoming Adverse Solubility Properties. *Organometallics* **2008**, *27*, 4772-4778. (b) Deacon, G. B.; Jaroschik, F.; Junk, P. C.; Kelly, R. P. A divalent heteroleptic lanthanoid fluoride complex stabilised by the tetraphenylcyclopentadienyl ligand, arising from C–F activation of pentafluorobenzene. *Chem. Commun.* **2014**, *50*, 10655-10657. (c) Kelly, R. P.; Bell, T. D. M.; Cox, R. P.; Daniels, D. P.; Deacon, G. B.; Jaroschik, F.; Junk, P. C.; Le Goff, X. F.; Lemercier, G.; Martinez, A.; Wang, J.; Werner, D. Divalent tetra- and pentaphenylcyclopentadienyl europium and samarium sandwich and half-sandwich complexes: synthesis, characterization and remarkable luminescence properties. *Organometallics* **2015**, *34*, 5624-5636. (d) Shephard, A. C. G.; Daniel, D. P.; Deacon, G. B.; Guo, Z.; Jaroschik, F.; Junk, P. C. Selective carbon-phosphorus bond cleavage: expanding the toolbox for accessing bulky divalent lanthanide sandwich

complexes. *Chem. Commun.* **2022**, *58*, 4344-4347. (e) Ruspic, C.; Moss, J. R.; Schürmann, M.; Harder, S. Remarkable Stability of Metallocenes with Superbulky Ligands: Spontaneous Reduction of Sm^{III} to Sm^{II}. *Angew. Chem. Int. Ed.* **2008**, *47*, 2121-2126. (f) Harder, S.; Naglav, D.; Ruspic, C.; Wickleder, C.; Adlung, M.; Hermes, W.; Eul, M.; Pöttgen, R.; Rego, D. B.; Poineau, F.; Czerwinski, K. R.; Herber, R. H.; Nowik, I. *Chem. - Eur. J.* **2013**, *19*, 12272−12280. (g) Van Velzen, N. J. C.; S. Harder, S. Deca-Arylsamarocene: An Unusually Inert Sm(II) Sandwich Complex. *Organometallics* **2018**, *37*, 2263;

(14) (a) Wang, Y.; Cheng, J. Half-sandwich scandium dibenzyl complexes bearing penta- or tetra-arylcyclopentadienyl ligands: synthesis, structure and syndiospecific styrene polymerization activity. *New J. Chem.* **2020**, *44*, 17333-17340. (b) Bardonov, D. A.; P. D. Komarov, P. D.; Ovchinnikova, V. I.; Puntus, L. N.; Minyaev, M. E.; Nifant'ev, I. E.; Lyssenko, K. A.; Korshunov, V. M.; Taidakov, I. V.; Roitershtein, D. M. Accessing Mononuclear Triphenylcyclopentadienyl Lanthanide Complexes by Using Tridentate Nitrogen Ligands: Synthesis, Structure, Luminescence, and Catalysis. *Organometallics* **2021**, *40*, 1235–1243. (c) Roitershtein, D. M.; Puntus, L. N.; Vinogradov, A. A.; Lyssenko, K. A.; Minyaev, M. E.; Dobrokhodov, M. D.; Taidakov, I. V.; Varaksina, E. A.; Churakov, A. V.; Nifant'ev, I. E. Polyphenylcyclopentadienyl Ligands as an Effective Light-Harvesting π-Bonded Antenna for Lanthanide +3 Ions. *Inorg. Chem.* **2018**, *57*, 10199–10213. (d) Arumugam, S.; Reddy, P. G.; Francis, M.; Kulkarni, A.; Roy, S.; Mondal, K. C. Highly fluorescent aryl-cyclopentadienyl ligands and their tetra-nuclear mixed metallic potassium–dysprosium clusters. *RSC Adv.* **2020**, *10*, 39366–39372.

(15) (a) Dilthey, W.; Huchtemann, P. Highly arylated compounds. IX. Highly arylated fulvenes. *J. Prakt. Chem.* **1940**, *154*, 238-265. (b) Dhar, D. N.; Ragunathan, R. Synthesis of spiropyrazolines: reaction of 1,3-diphenylnitrilimine with fulvenes. *Tetrahedron* **1984**, *40*, 1585-1590. (c) Debaerdemaeker, T.; Schroeer, W. D.; Friedrichsen, W. Reactions of fulvenes

with 1,3-dipolar compounds. III. Reactions of tetraarylfulvenes with 3-methyl-2,4-diphenyl-1,3-oxazolium-5-olat. *Liebigs Ann.* **1981**, 502-520. (d) Taber, D.; Becker, E. I.; Spoerri, P. E. The addition of bases to polar hydrocarbons. I. Reversal of the Mannich reaction. *J. Am. Chem. Soc*. **1954**, *76*, 776-781. (e) Drews, R.; Behrens, U. Transition metal fulvene complexes. XXIII. Tricarbonylfulvene and tricarbonylcyclopentadienyl complexes of molybdenum and tungsten. *Chem. Ber*. **1985**, *118*, 888-894.

(16) CrysAlisPRO v.55. Agilent Technologies Ltd., Yarnton, Oxfordshire, England.

(17) Sheldrick, G. M. Crystal structure refinement with SHELXL. *Acta Crystallogr. Sect. C Struct. Chem.* **2015**, *71*, 3–8.

(18) Barbour, L. J. X-Seed — A Software Tool for Supramolecular Crystallography. *J. Supramol. Chem.* **2001**, *1*, 189–191.

(19) (a) Hashimoto, H.; Tobita, H.; Ogino, H. Synthesis of the 1,2,3,4-Tetramethylfulvene-Bridged Diiron Complex (η^1:η^5-$CH_2C_5Me_4$)$Fe_2(CO)_6$ and Its Reactions with Phosphines. *Organometallics* **1993**, *12*, 2182−2187. (b) Döring, S.; Erker, G. Preparation of 1,2,3,4-Tetramethylpentafulvene by Hydride Anion Abstraction from Lithium Pentamethylcyclopentadienide Employing Tritylchloride. *Synthesis* **2001**, 43−45.

(20) Martin-Matute, B.; Edin, M.; Bogar, K.; Kaynak, F. B.; Baeckvall, J.-E. Combined Ruthenium(II) and Lipase Catalysis for Efficient Dynamic Kinetic Resolution of Secondary Alcohols. Insight into the Racemization Mechanism. *J. Am. Chem. Soc.* **2005**, *127*, 8817-8825.

(21) (a) Dyker, G.; Heiermann, J.; Miura, M.; Inoh, J.-I.; Pivsa-Art, S.; Satoh, T.; Nomura, M. Palladium-catalyzed arylation of cyclopentadienes. *Chem. Eur. J.* **2000**, *6*, 3426-3433. (b) Miura, M.; Pivsa-Art, S.; Dyker, G.; Heiermann, J.; Satoh, T.; Nomura, M. Palladium-catalyzed

reaction of aryl bromides with metallocenes to produce pentaarylated cyclopentadienes. *Chem. Commun.* **1998**, 1889-1890.

(22) (a) Baron, P.; Brown, R. D.; Burden, F. R.; Domaille, P.; Kent, J. The Microwave Spectrum and Structure of Fulvene. *J. Mol. Spectrosc.* **1972**, *43*, 401−410. (b) Meuche, D.; Neuenschwander, M.; Schaltegger, H.; Schlunegger, H. U. Fulven. *Helv. Chim. Acta* **1964**, *47*, 1211−1215. (c) Hollenstein, R.; von Philipsborn, W.; Vögeli, R.; Neuenschwander, M. Fulvene, VII. Analyse Der 13C- Und 1H-NMR.-Spektren. *Helv. Chim. Acta* **1973**, *56*, 847–860.

(23) Andrew, T. L.; Cox, J. R.; Swager, T. M. Synthesis, Reactivity, and Electronic Properties of 6,6-Dicyanofulvenes. *Org. Lett.* **2010**, *12*, 5302−5305.

(24) (a) Tatemura, R.; Yasutake, M.; Kinoshita, H.; Miura, K. Electrochemical Properties and Electrochromism of 6-Aryl-1,3-Bis(Trimethylsilyl)Fulvenes and Their Derivatives. *J. Org. Chem.* **2022**, *87*, 172–183. (b) Peloquin, A. J.; Stone, R. L.; Avila, S. E.; Rudico, E. R.; Horn, C. B.; Gardner, K. A.; Ball, D. W.; Johnson, J. E. B.; Iacono, S. T.; Balaich, G. J. Synthesis of 1,3-Diphenyl-6-Alkyl/Aryl-Substituted Fulvene Chromophores: Observation of π–π Interactions in a 6-Pyrene-Substituted 1,3-Diphenylfulvene. *J. Org. Chem.* **2012**, *77*, 6371–6376.

(25) Wu, G.; Rheingold, A. L.; Geib, S. J.; Heck, R. F. Palladium-catalyzed annulation of aryl iodides with diphenylacetylene. *Organometallics* **1987**, *6*, 1941-1946.

(26) Hitchcock, P. B.; Lappert, M. F.; Tian, S. Lanthanocene Chemistry with $[Cp^R]^-$, $[Cp^t]$, $[Cp^{tt}]^-$, and $[Cp^{R'}{}_2SiMe_2]^{2-}$ Ligands: Synthesis and Characterization of Bis(cyclopentadienyl)lanthanide(III) Halides and Bis(cyclopentadienyl)lanthanide(II) Complexes and Crystal Structures of $[\{NdCp^R{}_2(\mu\text{-}Cl)\}_2]$, $[\{TmCp^{tt}{}_2(\mu\text{-}I)\}_2]$,and $[Yb(Cp^{R'}{}_2SiMe_2)(THF)_2]$ ($Cp^R = \eta^5\text{-}C_5H_4\{CH(SiMe_3)_2\}$,$Cp^t = \eta^5\text{-}C_5H_4(SiMe_2But)$, $Cp^{tt} = \eta^5$-

$C_5H_3(SiMe_2But)_2$-1,3,and $Cp^{R'}$ = η^5-$C_5H_3\{CH(SiMe_3)_2\}$-3). *Organometallics* **2000,** *19,* 3420-3428 and references therein.

(27) (a) Higashiyama, N.; Takemura, K.; Kimura, K.; Adachi, G.-Y. Luminescence of divalent europium complexes with N-pivot lariat azacrown ethers. *Inorg. Chim. Acta* **1992**, *194*, 201−206. (b) Jenks, T. C.; Bailey, M. D.; Corbin, B. A.; Kuda-Wedagedara, A. N. W.; Martin, P. D.; Schlegel, H. B.; Rabuffetti, F. A.; Allen, M. J. Photophysical Characterization of a Highly Luminescent Divalent-Europium-Containing Azacryptate. *Chem. Commun.* **2018**, *54*, 4545–4548. (c) Ekanger, L. A.; Mills, D. R.; Ali, M. M.; Polin, L. A.; Shen, Y.; Haacke, E. M.; Allen, M. J. Spectroscopic Characterization of the 3+ and 2+ Oxidation States of Europium in a Macrocyclic Tetraglycinate Complex. *Inorg. Chem.* **2016**, *55*, 9981–9988. (d) Poe, T. N.; Beltrán-Leiva, M. J.; Celis-Barros, C.; Nelson, W. L.; Sperling, J. M.; Baumbach, R. E.; Ramanantoanina, H.; Speldrich, M.; Albrecht-Schönzart, T. E. Understanding the Stabilization and Tunability of Divalent Europium 2.2.2B Cryptates. *Inorg. Chem.* **2021**, *60*, 7815–7826. (e) Simler, T.; Feuerstein, T. J.; Yadav, R.; Gamer, M. T.; Roesky, P. W. Access to Divalent Lanthanide NHC Complexes by Redox-Transmetallation from Silver and CO_2 Insertion Reactions. *Chem. Commun.* **2019**, *55*, 222–225. (f) Sitzmann, H.; Dezember, T.; Schmitt, O.; Weber, F.; Wolmershäuser, G.; Ruck, M. Metallocenes of Samarium, Europium, and Ytterbium with the Especially Bulky Cyclopentadienyl Ligands $C_5H(CHMe_2)_4$, $C_5H_2(CMe_3)_3$, and $C_5(CHMe_2)_5$. *Z. Anorg. Allg. Chem.* **2000**, *626*, 2241−2244. (g) Thomas, A. C.; Ellis, A. B. Diethyl ether adducts of bis(pentamethylcyclopentadienyl) europium(II) and -ytterbium(II). Excited-state energy transfer with organolanthanoid complexes. *Organometallics* **1985**, *4*, 2223−2225. (h) Kawasaki, K.; Sugiyama, R.; Tsuji, T.; Iwasa, T.; Tsunoyama, H.; Mizuhata, Y.; Tokitoh, N.; Nakajima, A. A Designer Ligand Field for Blue-Green Luminescence of Organoeuropium(II) Sandwich Complexes with Cyclononatetraenyl Ligands. *Chem. Commun.* **2017**, *53*, 6557–6560. (i) Suta, M.; Kühling, M.; Liebing, P.; Edelmann, F. T.; Wickleder, C.

Photoluminescence Properties of the "Bent Sandwich-like" Compounds [Eu(Tp^{IPr2})$_2$] and [Yb(TpI^{Pr2})$_2$] – Intermediates between Nitride-Based Phosphors and Metallocenes. *J. Lumin.* **2017**, *187*, 62–68. (j) Qi, H.; Zhao, Z.; Zhan, G.; Sun, B.; Yan, W.; Wang, C.; Wang, L.; Liu, Z.; Bian, Z.; Huang, C. Air Stable and Efficient Rare Earth Eu(II) Hydro-Tris(Pyrazolyl)Borate Complexes with Tunable Emission Colors. *Inorg. Chem. Front.* **2020**, *7*, 4593–4599. (k) Goodwin, C. A. P.; Chilton, N. F.; Vettese, G. F.; Moreno Pineda, E.; Crowe, I. F.; Ziller, J. W.; Winpenny, R. E. P.; Evans, W. J.; Mills, D. P. Physicochemical Properties of Near-Linear Lanthanide(II) Bis(Silylamide) Complexes (Ln = Sm, Eu, Tm, Yb). *Inorg. Chem.* **2016**, *55*, 10057–10067. (l) Goodwin, C. A. P.; Chilton, N. F.; Natrajan, L. S.; Boulon, M.-E.; Ziller, J. W.; Evans, W. J.; Mills, D. P. Investigation into the Effects of a Trigonal-Planar Ligand Field on the Electronic Properties of Lanthanide(II) Tris(Silylamide) Complexes (Ln = Sm, Eu, Tm, Yb). *Inorg. Chem.* **2017**, *56*, 5959–5970.

(28) (a) Galimov, D. I.; Bulgakov, R. G. The First Example of Fluorescence of the Solid Individual Compounds of Eu^{2+} Ion: $EuCl_2$, EuI_2 , $EuBr_2$. *Luminescence* **2019**, *34*, 127–129. (b) Marks, S.; Heck, J. G.; Habicht, M. H.; Oña-Burgos, P.; Feldmann, C.; Roesky, P. W. [Ln(BH_4)$_2$(THF)$_2$] (Ln = Eu, Yb) - A Highly Luminescent Material. Synthesis, Properties, Reactivity, and NMR Studies. *J. Am. Chem. Soc.* **2012**, *134*, 16983–16986. (c) Galimov, D. I.; Yakupova, S. M.; Vasilyuk, K. S.; Sabirov, D. S.; Bulgakov, R. G. Effect of Coordination Environment of Eu^{2+} Ion on the 5d-4f Luminescence of Molecular Compounds EuL_2(THF) (L = Cl, Br, I, NO_3, Ac, Fod, Tmhd, and Acac; x = 0, 2). *J. Photochem. Photobiol. Chem.* **2020**, *403*, 112839. (d) Starynowicz, P. Complexes of Divalent Europium with Dotp and Dotpph. *New J. Chem.* **2021**, *45*, 5879–5889. (e) Straub, L. C.; Adlung, M.; Wickleder, C.; Wickleder, M. S.; Rasche, B. Impact of 1,10-Phenanthroline-Induced Intermediate Valence on the Luminescence of Divalent Europium Halides. *Inorg. Chem.* **2023**, *62*, 497–507.

(29) (a) Qiao, J.; Ning, L.; Molokeev, M. S.; Chuang, Y.-C.; Liu, Q.; Xia, Z. Eu^{2+} Site Preferences in the Mixed Cation $K_2BaCa(PO_4)_2$ and Thermally Stable Luminescence. *J. Am. Chem. Soc.* **2018**, *140*, 9730–9736. (b) Gehlhaar, F.; Finger, R.; Zapp, N.; Bertmer, M.; Kohlmann, H. $LiSr_2SiO_4H$, an Air-Stable Hydride as Host for Eu(II) Luminescence. *Inorg. Chem.* **2018**, *57*, 11851–11854. (c) Lai, S.; Zhao, M.; Zhao, Y.; Molokeev, M. S.; Xia, Z. Eu^{2+} Doping Concentration-Induced Site-Selective Occupation and Photoluminescence Tuning in $KSrScSi_2O_7$:Eu^{2+} Phosphor. *ACS Mater. Au* **2022**, *2*, 374–380.

(30) (a) Barraza, R.; Allen, M. Lanthanide Luminescence in Visible-Light-Promoted Photochemical Reactions. *Molecules* **2020**, *25*, 3892. (b) Galimov, D. I.; Yakupova, S. M.; Vasilyuk, K. S.; Bulgakov, R. G. A Novel Gas Assay for Ultra-Small Amounts of Molecular Oxygen Based on the Chemiluminescence of Divalent Europium. *J. Photochem. Photobiol. Chem.* **2021**, *418*, 113430. (c) Tang, Z.; Zhang, Q.; Cao, Y.; Li, Y.; Wang, Y. Eu^{2+}-Doped Ultra-Broadband VIS-NIR Emitting Phosphor. *Chem. Eng. J.* **2020**, *388*, 124231. (d) Feng, P.-F.; Kong, M.-Y.; Yang, Y.-W.; Su, P.-R.; Shan, C.-F.; Yang, X.-X.; Cao, J.; Liu, W.-S.; Feng, W.; Tang, Y. Eu^{2+}/Eu^{3+}-Based Smart Duplicate Responsive Stimuli and Time-Gated Nanohybrid for Optical Recording and Encryption. *ACS Appl. Mater. Interfaces* **2019**, *11*, 1247–1253. (e) Jenks, T. C.; Bailey, M. D.; Hovey, J. L.; Fernando, S.; Basnayake, G.; Cross, M. E.; Li, W.; Allen, M. J. First Use of a Divalent Lanthanide for Visible-Light-Promoted Photoredox Catalysis. *Chem. Sci.* **2018**, *9*, 1273–1278. (f) Barraza Jr., R.; Sertage, A. G.; Kajjam, A. B.; Ward, C. L.; Lutter, J. C.; Schlegel, H. B.; Allen, M. J. Properties of Amine-Containing Ligands That Are Necessary for Visible-Light-Promoted Catalysis with Divalent Europium. *Inorg. Chem.* **2022**, *61*, 19649–19657. (g) Galimov, D. I.; Yakupova, S. M.; Bulgakov, R. G. Divalent Eu^{2+} Ion - an Effective Inorganic Mediator of Energy Transfer from the Primary Chemiluminescence Emitter $^3Me_2CHC(H)=O^*$ on Tb^{3+} and $Ru(Bpy)_3^{2+}$ Ions. *Luminescence* **2018**, *33*, 1365–1370. (h) Li, J.; Wang, L.; Zhao, Z.; Sun, B.; Zhan, G.; Liu, H.;

Bian, Z.; Liu, Z. Highly Efficient and Air-Stable Eu(II)-Containing Azacryptates Ready for Organic Light-Emitting Diodes. *Nat. Commun.* **2020**, *11*, 5218.

(31) (a) Dorenbos, P. Energy of the First $4f^7 \rightarrow 4f^6 5d$ Transition of Eu^{2+} in Inorganic Compounds. *J. Lumin.* **2003**, *104*, 239–260. (b) Dorenbos, P. F d Transition Energies of Divalent Lanthanides in Inorganic Compounds. *J. Phys. Condens. Matter* **2003**, *15*, 575–594.

(32) (a) Acharjya, A.; Corbin, B. A.; Prasad, E.; Allen, M. J.; Maity, S. Solvation-Controlled Emission of Divalent Europium Salts. *J. Photochem. Photobiol. Chem.* **2022**, *429*, 113892. (b) Basal, L. A.; Kajjam, A. B.; Bailey, M. D.; Allen, M. J. Systematic Tuning of the Optical Properties of Discrete Complexes of Eu^{II} in Solution Using Counterions and Solvents. *Inorg. Chem.* **2020**, *59*, 9476–9480.

(33) (a) Diaz-Rodriguez, R. M.; Gálico, D. A.; Chartrand, D.; Suturina, E. A.; Murugesu, M. Toward Opto-Structural Correlation to Investigate Luminescence Thermometry in an Organometallic Eu(II) Complex. *J. Am. Chem. Soc*. **2022**, *144*, 912−921. (b) Ilichev, V. A.; Silantyeva, L. I.; Rogozhin, A. F.; Yablonskiy, A. N.; Andreev, B. A.; Rumyantsev, R. V.; Fukina, G. K.; Bochkarev, M. N. Luminescence thermochromism in novel mixed Eu(II)–Cu(I) iodide. *Dalton Trans.* **2021**, *50*, 14244-14251.

(34) Cowieson, N. P.; Aragao, D.; Clift, M.; Ericsson, D. J.; Gee, C.; Harrop, S. J.; Mudie, N.; Panjikar, S.; Price, J. R.; Riboldi-Tunnicliffe, A.; Williamson R.; Caradoc-Davies, T. *J. Synchrotron Radiat.* **2015**, *22*, 187-190.

“For Table of Contents Only”

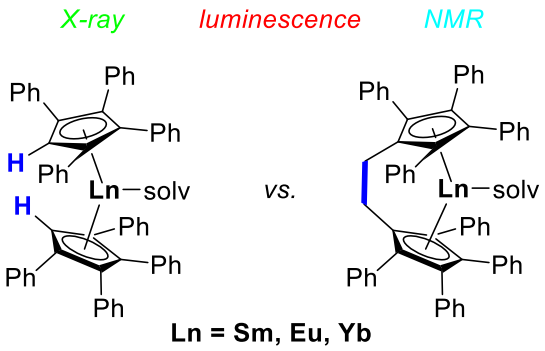

Synopsis : New divalent *ansa*-octaphenyllanthanocene complexes were synthesised by reductive dimerisation of 1,2,3,4-tetraphenylfulvene and their X-ray structures and spectroscopic properties (multinuclear NMR spectroscopy, luminescence) compared to unbridged octaphenyl and decaphenyl sandwich complexes.